The Selective Carbochlorination of Iron from Titaniferous Magnetite Ore in a Fluidized Bed

K.I. RHEE and H.Y. SOHN

The selective chlorination of iron from titaniferous magnetite ore using solid carbon as a reducing agent was studied in a fluidized bed. The effects of chlorination temperature, chlorine gas partial pressure, ratio of ore to carbon particle sizes, and the amount of added carbon were determined. Experimental results indicate that temperatures between 900 and 1000 K were favorable for the selective chlorination of iron. The rate was found to be first order with respect to chlorine concentration, and the observed effects of particle size, temperature, and the amount of carbon added were expressed quantitatively by using a mixed-control model.

I. INTRODUCTION

TITANIFEROUS magnetite is one of the most abundant and widespread titanium-bearing minerals. It can be used for producing titanium metal and titanium dioxide through the chlorination process. Due to the high content of impurities in these minerals, especially iron, it is necessary to upgrade them to obtain synthetic rutile, which is acceptable as a feedstock for chlorination. A number of processes[1–5] have been proposed for the removal of iron from a low-grade titanium ore, such as chlorination by various agents with or without pretreatment, smelting followed by sulfation and hydrochloric acid leaching, hydrogen reduction followed by ferric salt leaching, high-temperature/high-pressure leaching with sulfuric acid in the presence of a reducing agent, and solid-state reduction followed by chemical or physical separation.

Among these processes, the direct chlorination has a significant advantage in that it can be done in conventional chlorination equipment and requires no other pretreatment such as roasting or slagging. Some operational difficulties are, however, associated with this process due to the defluidization and clogging caused by high-boiling-point metal chlorides produced during chlorination. Nonetheless, these difficulties can be removed by the control of temperature, amount of reducing agent, and the partial pressure of chlorine.

Usually, direct chlorination can be accomplished in two ways. One is the chlorination of both iron and titanium, forming volatile chlorides which are subsequently separated. The other is the selective chlorination of iron in the ore, leaving a titanium oxide-rich residue. The selective chlorination also has the advantages of increasing the efficiency of chlorine consumption and requiring lower energy, because the chlorination of iron is thermodynamically more favorable than that of titanium. In addition, iron removal from titaniferous ore results in greatly increased porosity and surface area, and thus, the reactivity of this beneficiated ore is generally high.[6]

An industrial chlorination process will likely use carbon as a reducing agent instead of carbon monoxide gas, because solid carbon is well known to be the more effective reductant. Morris and Jensen[7] reported that the rate of the chlorination of rutile by carbon was much faster than that by carbon monoxide, and Bergholm[8] explained the reactivity of these reducing agents based on the dependency of partial pressures of chlorine and carbon monoxide gas on the chlorination rates of Australian rutile.

Despite a number of investigations[9–13] on the selective chlorination of low-grade titanium-bearing ores, the carbochlorination of titaniferous magnetite ore has not been reported in the literature. In the present study, the kinetics of the selective chlorination of iron from titaniferous magnetite ore were determined in a fluidized bed. Experiments were conducted to determine the effects of chlorination temperature, chlorine partial pressure, particle sizes of ore and carbon, and the amount of added carbon.

II. EXPERIMENTAL

A. *Sample Preparation*

The titaniferous magnetite ore used in these experiments came from Soyunpyung-Do, Korea. This ore was ground and sieved into various size fractions of 74 to 149 μm, and representative samples were fused with lithium metaborate and dissolved in a 0.5 N HCl solution. The resulting solution was analyzed using a direct current plasma (DCP) spectrometer. Table I shows the chemical composition of this ore.

Ilmenite and magnetite were the predominant phases, and quartz and silicates were the minor phases identified by X-ray diffraction (Table II).

Activated carbon, with 98 wt pct fixed carbon and a maximum of 2 wt pct ash, was used as the reducing agent. To avoid the segregation of the ore and the carbon in the extended bed, a proper particle-size ratio had to be chosen that takes into account the density difference between the two solids. This will be discussed in detail in Section III.

B. *Apparatus and Procedure*

The fluidized bed reactor shown in Figure 1 consisted of a quartz tube, 5 cm in diameter and 70 cm in length,

K.I. RHEE, formerly Graduate Student with the Department of Metallurgical Engineering, University of Utah, is Head of Rare Metals Research Department, Korea Institute of Energy and Resources, Daejeon, Korea. H.Y. SOHN, Professor, is with the Department of Metallurgical Engineering, University of Utah, Salt Lake City, UT 84112-1183.

Manuscript submitted March 21, 1989.

Table I. Chemical Analysis of Titaniferous Magnetite

Component	Content, Wt Pct
TiO_2	20.2
FeO	21.4
Fe^{3+} as Fe_2O_3*	44.6
SiO_2	2.63
MgO	4.01
Al_2O_3	3.18

*For analytical procedure, the reader is referred to Ref. 12.

Table II. X-Ray Diffraction Analysis of Titaniferous Magnetite

Mineral	Occurrence
Ilmenite ($FeTiO_3$)	major
Magnetite (Fe_3O_4)	major
Quartz (SiO_2)	minor
Unidentified	minor

inside which a porous fritted disc to be used as a gas distributor was welded. A sampling tube was connected to this reactor and was situated at the top of the bed. The reactor was externally heated by a silicon carbide furnace which was controlled by a temperature controller using a Pt-13 pct Rh thermocouple. Temperature during the reaction was measured by a CHROMEL-ALUMEL* thermocouple immersed in the expanded bed. The connecting tube was wrapped with heating tape and maintained at 623 K in order to avoid plugging and was connected to a receptacle for ferric chloride and then to an absorption bubble column containing sodium hydroxide solution.

*CHROMEL-ALUMEL is a trademark of Hoskins Manufacturing Company, Hamburg, MI.

Weighed amounts of the ore and carbon were charged into the preheated reactor, while a flow of nitrogen was continued in order to keep the mixture in a fluidized state and to avoid oxidation. When the temperature reached the desired value, the nitrogen flow was discontinued, and a calibrated flow of Cl_2/N_2 mixture was passed through both the gas distributor and the sampling tube. Partially reacted ore mixture was withdrawn through the sampling tube at regular time intervals. Ore residue was screened from each sample, weighed, and subjected to chemical analysis.

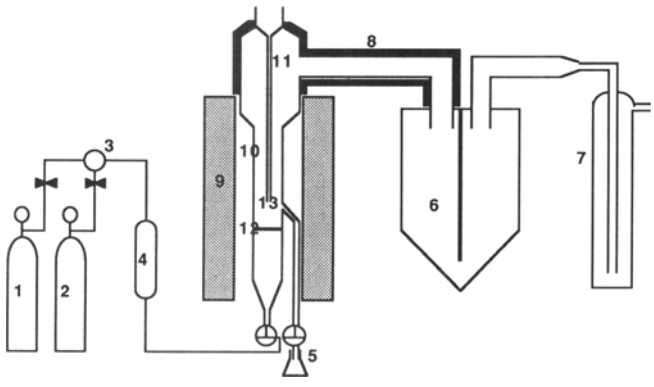

Fig. 1—Schematic diagram of experimental apparatus for carbo-chlorination: (1) chlorine cylinder; (2) nitrogen cylinder; (3) gas control system; (4) rotameter; (5) sampling device; (6) receptacle; (7) NaOH bubbler; (8) heating tape; (9) furnace; (10) reactor; (11) thermocouple; (12) gas distributor; and (13) solid reactants.

III. RESULTS AND DISCUSSION

Figure 2 shows the selectivity of iron chlorination from various titanium-bearing ores (*i.e.*, mainly ilmenite and magnetite phases in raw titaniferous magnetite; pseudobrookite, rutile, and hematite phases in an oxidized ore; and ilmenite in the nonmagnetic fraction from magnetic separation). This figure shows that the titaniferous magnetite ore resulted in a high ratio of chlorinated Fe to chlorinated Ti.

As shown in Figure 3, the overall rate of titanium and iron chlorination increases with increasing temperature, but the rate of titanium chlorination increases more rapidly with temperature than that of iron chlorination. Therefore, the selective chlorination must be carried out below 973 K if titanium chlorination needs to be kept below 10 pct when most of the iron is chlorinated.

Photomicrographs of the partially chlorinated ore, obtained using light microscopy, are shown in Figure 4. A clear boundary between the outer TiO_2 product layer and the inner unreacted core can be observed in the optical microscopic structures. As the conversion increases, the product layer thickness increases, while the overall particle size remains unchanged. It is apparent that this system displays the attributes of a typical unreacted shrinking-core model.

Since various iron oxides are present in titaniferous magnetite ore, a rigorous determination of the degree of chlorination for each oxide is difficult. Based on the stoichiometry of the chemical reaction of each oxide, the amount of chlorine required can be calculated. Thus, the amounts of chlorine required per gram of FeO, Fe_3O_4, and Fe_2O_3 are 1.48, 1.38, and 1.33 g, respectively. Using the chemical composition of the ore, the error introduced by assuming the iron to be present entirely as Fe_2O_3 is

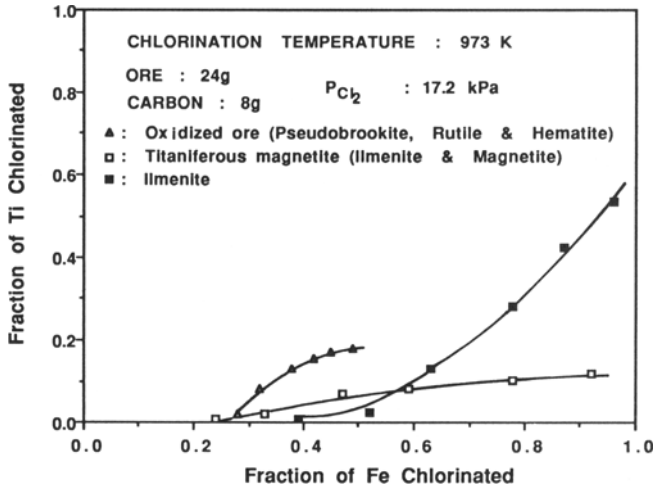

Fig. 2—Comparison of iron and titanium chlorination from various ore phases in carbon-chlorine system.

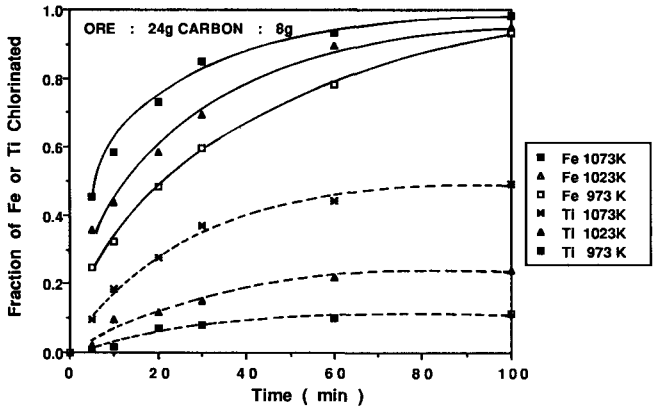

Fig. 3—Effect of temperature on iron and titanium chlorination from titaniferous magnetite ore. (——— Fe; ––– Ti)

3.1 pct, when iron oxide in this ore is completely chlorinated. In addition to this assumption, various other chemical reactions take place in the chlorination of titaniferous magnetite, *i.e.*, complicated reactions involving carbon, side reactions by the metal chlorides produced, and volatilization of the metal chlorides. For this reason, it is very difficult to analyze the fundamental kinetics of chlorination of this titaniferous magnetite ore.

Furthermore, mixing/segregation becomes important when more than one solid is involved in a fluidized bed reactor. Many investigations on binary mixtures in fluidization have been made. Among these, Nienow *et al.*[14] developed an empirical relationship, as shown in the following Eq. [1], considering the hydrodynamic effect, physical properties (density and sphericity), and operating conditions (bed height, bed diameter, and ratio of two solid quantities), which is in good agreement with experimental measurements:

$$M = \left[1 + \exp\left\{-\left(\frac{U - U_{TO}}{U - U_F}\right)\exp\left(\frac{U}{U_{TO}}\right)\right\}\right]^{-1} \quad [1]$$

where

$$U_{TO} = U_F\left[\left(\frac{U_P}{U_F}\right)^{1.2} + 0.9\left(\frac{\rho_H}{\rho_L} - 1\right)^{1.1}\left(\frac{\phi_H d_H}{\phi_L d_L}\right)^{0.7} - 2.2\bar{x}^{0.5}\left\{1 - \exp\left(-\frac{H}{D}\right)\right\}^{1.4}\right]$$

where M = mixing index, $x/\bar{x}$ (complete mixing for $M = 1$ and complete segregation for $M = 0$)
D = bed diameter, mm
d_H = diameter of the heavier particle, mm
d_L = diameter of the lighter particle, mm
H = bed height, mm
U = superficial gas velocity, m/s
U_F = the U_{mf} of the component with the lower U_{mf}, m/s
U_P = the U_{mf} of the component with the higher U_{mf}, m/s
U_{mf} = minimum fluidization velocity in general, m/s
U_{TO} = the velocity above which mixing takes over ($U = U_{TO}$ at $M = 0.5$), m/s
x = mass fraction of the heavier particle in the upper uniform part of the bed
$\bar{x}$ = the overall mass fraction
ϕ_H = sphericity of the heavier particle
ϕ_L = sphericity of the lighter particle
ρ_H = density of the heavier particle, kg/m^3
ρ_L = density of the lighter particle, kg/m^3

Applying Eq. [1] to the carbon and titaniferous ore binary mixture with respective average diameters of 250 and 125 μm, M was 0.94 from the calculated value of 0.0398 m/s for U_{TO} when U was 0.0693 m/s (973 K and 86.1 kPa). This indicated that a flow rate of 2.5 l/min (298 K and 86.1 kPa) would give good mixing.

Nevertheless, exact quantitative analysis can only be accomplished by combining this empirical relationship with experiments on the actual system considered. Therefore, even though ore and carbon particle sizes were selected based on Eq. [1], some experiments to determine this mixing effect were performed.

The solid mixtures were withdrawn from the expanded bed using various nitrogen flow rates at the temperature considered for this system. After cooling, the sample was screened to separate ore from carbon. It was necessary to find the flow rate for which the ratio of ore to carbon in the withdrawn sample approaches the initially charged ratio. Results showed that the ratio remained constant above a flow rate of 2.5 l/min (298 K and 86.1 kPa). Based on this observation, a total flow rate of 3 l/min (298 K and 86.1 kPa) was used for subsequent experiments.

Variables Affecting the Chlorination of Titaniferous Magnetite

1. *Effect of chlorine partial pressure*

As mentioned in connection with the microscopic examination, the shrinking-core model can be used to explain the experimental data. Attempts were made to fit the overall experimental data using the model governed by either the chemical reaction or diffusion control, but neither of them could interpret the data. Hence, both steps need to be considered to obtain the rate expression. By introducing the law of additive time[15] expressed in Eq. [2], we can correlate the experimental conversion *vs* time data:

$$t = c_1 g_{F_p}(X) + c_2 p_{F_p}(X) \quad [2]$$

where

$$g_{F_p}(X) = 1 - (1 - X)^{1/3}$$

$$p_{F_p}(X) = 1 - 3(1 - X)^{2/3} + 2(1 - X)$$

and

$$c_1 \propto \frac{\rho_s r_p}{k C_A^n}; \qquad c_2 \propto \frac{\rho_s r_p^2}{D_e C_A}$$

where C_A = molar concentration of A
D_e = effective diffusivity
k = reaction rate constant

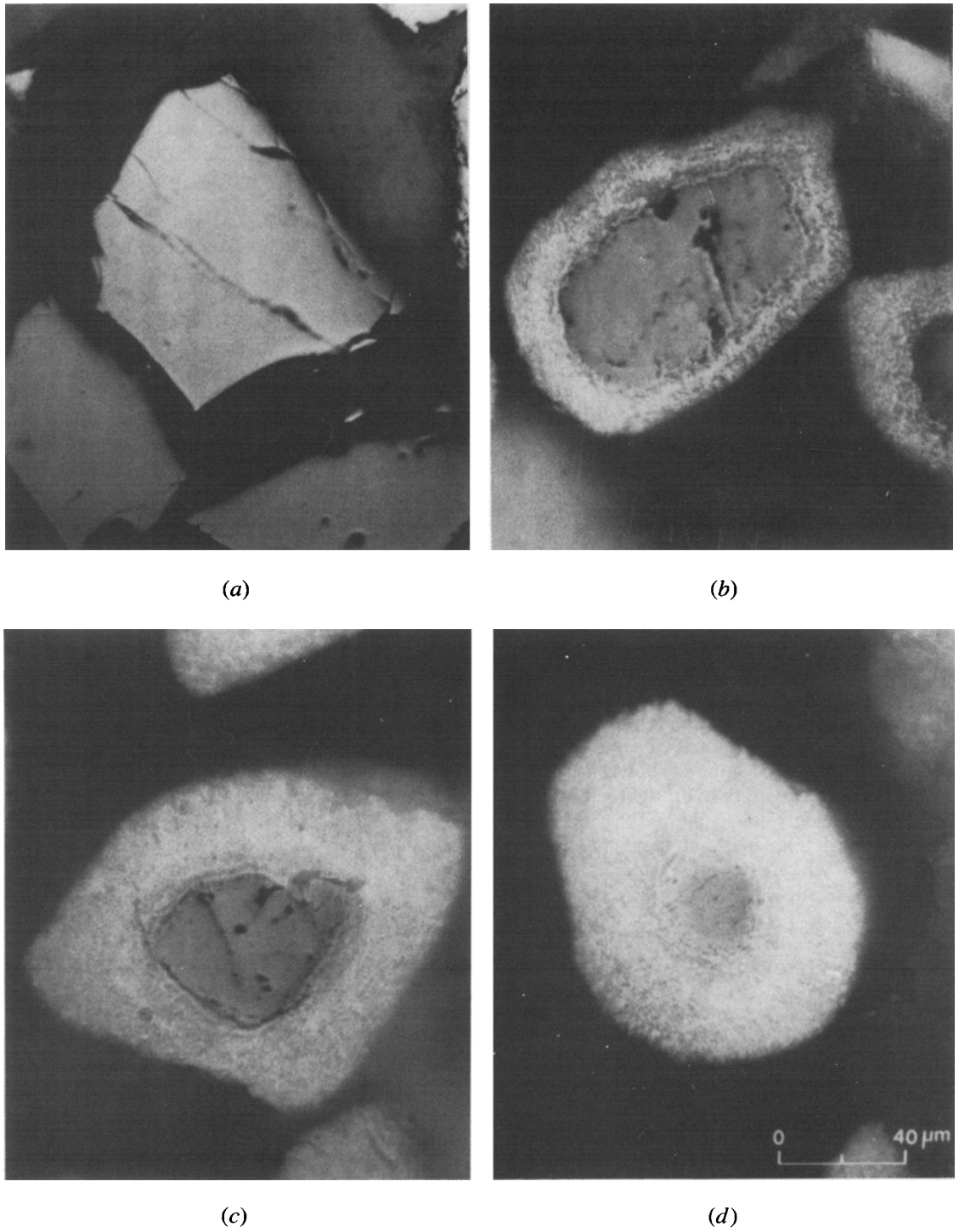

Fig. 4—Photomicrographs of cross section of particles: (*a*) original ore, (*b*) 51 pct conversion, (*c*) 76 pct conversion, and (*d*) 98 pct conversion.

n = reaction order with respect to gaseous reactant
r_p = original position of external surface
X = fractional conversion of the solid
ρ_s = molar concentration of solid reactant

Through the method of Nedler and Mead (flexible polyhedron search method as cited in Reference 16), c_1 and c_2 can be obtained from minimization of the following function:

$$\sum_{i=1}^{n} (\text{error})_i^2 = \sum_{i=1}^{n} (c_1 g_{F_p}(X_i) + c_2 p_{F_p}(X_i) - t_i)^2 \quad [3]$$

where n is the number of data points to be used. All computer solutions of c_1 and c_2 for different experimental conditions used are given in Table III. Using the values of c_1 and c_2 for different chlorine pressures, a

Table III. Values of c_1 and c_2 for Various Experimental Conditions

Variable		Variables Kept Constant	c_1	c_2
Chlorine gas	17.2 kPa	898 K	35.3	145.3
	28.7 kPa	96.0 μm ore and 177 μm C	51.2	217.9
	43.1 kPa	3.3:1 ore/C	85.3	363.2
Temperature	848 K	96.0 μm ore and 177 μm C	260.1	754.2
	898 K	17.2 kPa	85.3	363.2
	933 K	3.3:1, ore/C	45.1	231.0
	973 K		24.0	158.5
Ore particle size (carbon particle size)	80.7 μm (125 μm)	933 K	37.9	163.2
	96.0 μm (177 μm)	17.2 kPa	45.1	231.0
	125 μm (250 μm)	3.3:1, ore/C	58.7	391.6
Carbon added	10:1, ore/C	17.2 kPa	63.9	490.0
	5:1, ore/C	96.0 μm ore and 177 μm C	36.8	265.3
	3.3:1, ore/C	973 K	24.0	158.5

comparison of Eq. [2] with experimental data is presented in Figure 5. It is possible to determine the reaction order with respect to chlorine from the plot of ln c_1 *vs* ln C_{Cl_2}. Figure 6 indicates that the reaction is first order with respect to chlorine gas. However, this analysis must be considered approximate and global because the corresponding variation of CO pressure was not included.

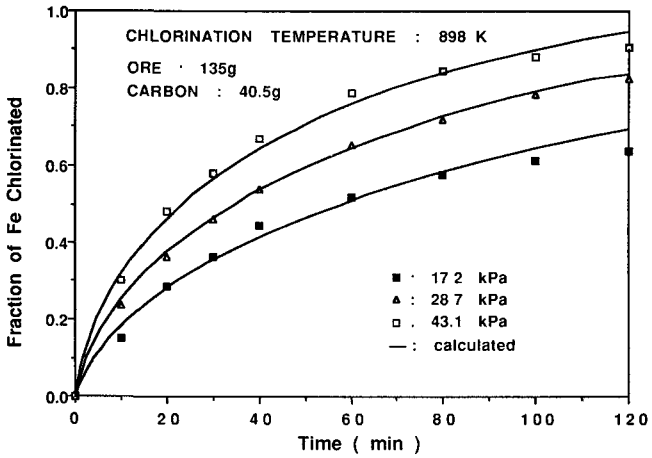

Fig. 5—Effect of the partial pressure of chlorine on the carbochlorination and comparison of experimental data with the values based on shrinking unreacted core model.

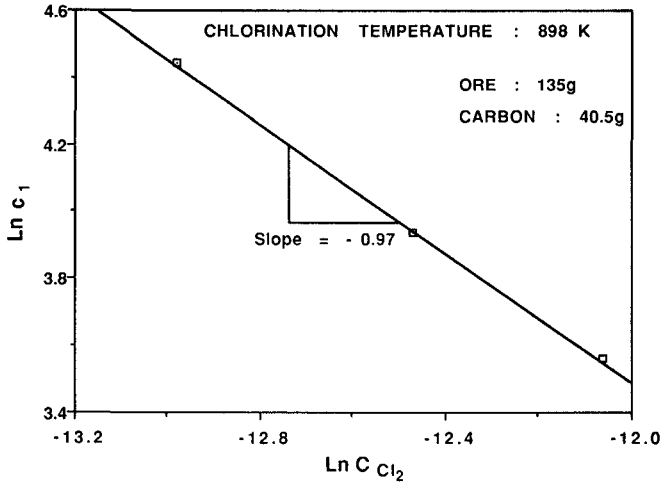

Fig. 6—Plot of ln c_1 *vs* ln C_{Cl_2} based on the model.

2. *Effect of particle size*

The chlorination curves of three different size fractions for both the ore and carbon (74 to 88 μm ore and 105 to 149 μm carbon, 88 to 105 μm ore and 149 to 210 μm carbon, 105 to 149 μm ore, and 210 to 297 μm carbon) are presented in Figure 7, which shows an increase of conversion with decreasing particle size. The calculated curves have been obtained using the same procedure described above. The proportionality of c_1 to r_p and c_2 to r_p^2, respectively, in Figure 8 further supports the idea that the chlorination in this system can be interpreted by a shrinking-core model affected by both the chemical reaction and diffusion through the product layer.

3. *Effect of temperature*

In order to investigate the effect of temperature on the chlorination rate, experiments were performed by varying the temperature in the range of 848 to 973 K. Experimental results and calculated values are presented in Figure 9. It is seen from Figure 10 that c_1 and c_2 have an Arrhenius-type relationship. Due to many diffusing

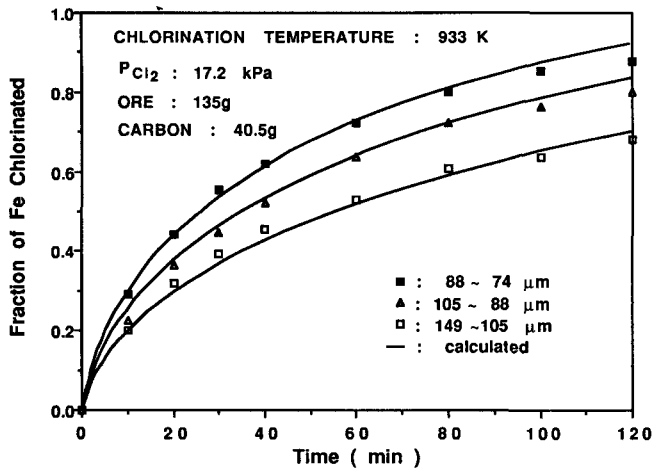

Fig. 7—Effect of particle size on the chlorination of titaniferous magnetite ore. (Ore particle sizes are indicated in the figure. The corresponding carbon particle sizes were 105 to 149 μm, 149 to 210 μm, and 210 to 297 μm.)

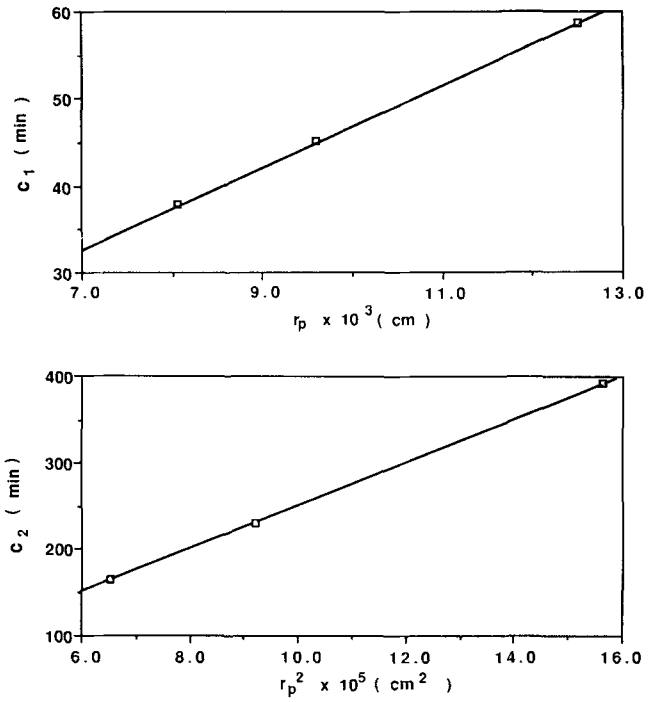

Fig. 8—Plots of c_1 *vs* r_p and c_2 *vs* r_p^2.

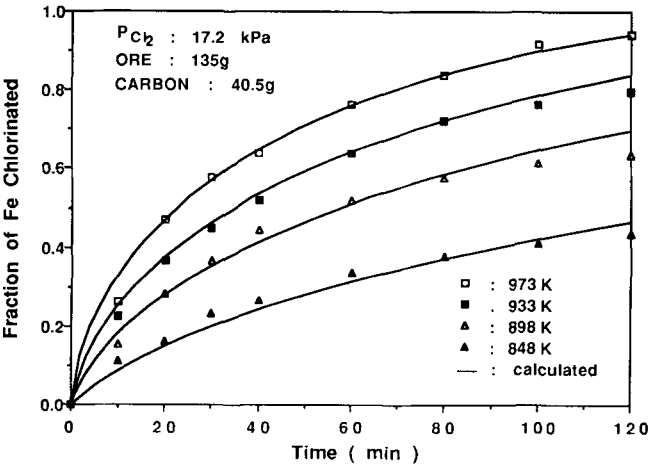

Fig. 9—Effect of temperature on the chlorination of titaniferous magnetite ore.

species involved, such as CO, CO_2, Cl_2, $FeCl_3$, and O_2, a rigorous interpretation of temperature dependency on the chlorination is difficult. However, apparent activation energies of 131 kJ/mol for the chemical reaction and 86 kJ/mol for diffusion were obtained.

4. *Effect of carbon content*

The effects of the amount of added carbon were determined by varying the ratio of ore to carbon while holding the bed height constant. Figure 11 shows that the calculated values using the same procedure fit the experimental results very well. The chlorination rate increases with increasing amount of carbon; however, a detailed reaction mechanism has not been attempted in this work. Future work will be needed for a systematic analysis of the effect of carbon content.

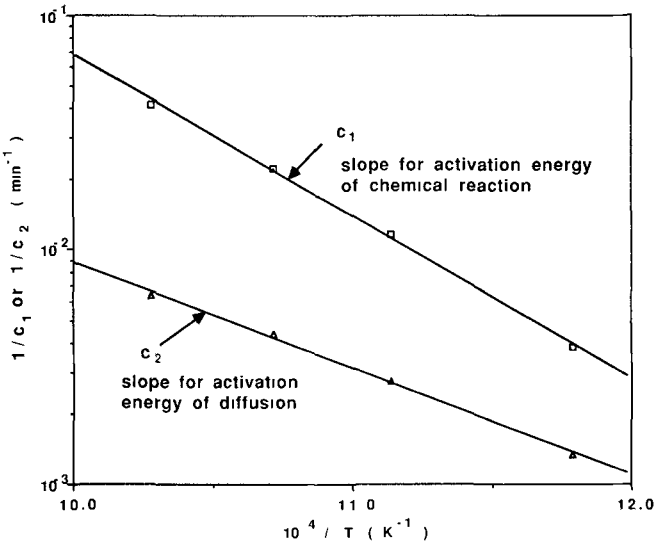

Fig. 10—Plot of ln $1/c_1$ and $1/c_2$ *vs* $1/T$.

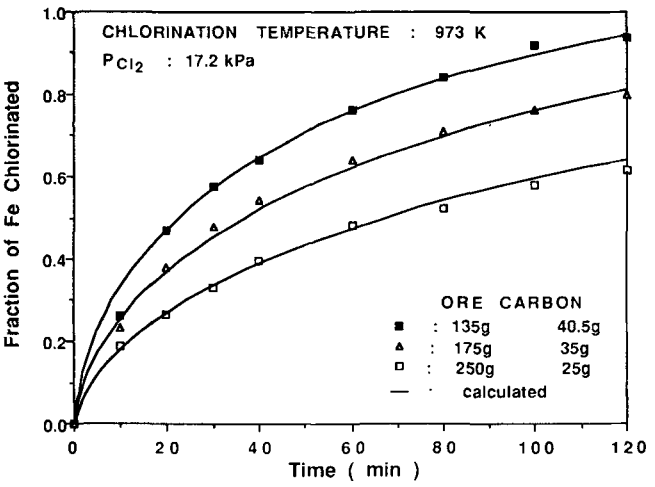

Fig. 11—Effect of the amount of carbon added on the chlorination of titaniferous magnetite ore.

IV. CONCLUSIONS

The effects of variables affecting the chlorination of titaniferous magnetite in a fluidized bed were investigated. Optimum conditions for selectivity of iron chlorination in terms of ore phase, temperature, carbon content, and particle-size ratio of ore to carbon were obtained from experiments. Temperatures between 900 and 1000 K, 33 wt pct carbon added, and an ore/carbon particle-size ratio of 0.5 gave the best results for the selective chlorination of the titaniferous magnetite sample used in this work.

The law of additive reaction times, which takes into account both chemical reaction and pore diffusion, was found to adequately describe the experimental data.

ACKNOWLEDGMENTS

The authors wish to thank Drs. S.J. Im and D. Kim, both formerly with the Korea Institute of Energy and

Resources, Daejeon, and now with Lucky Metals Corporation, Seoul, Korea, for many helpful discussions during the course of this work and for kindly supplying the low-grade titaniferous magnetite ore used in this work. This work was supported in part by the Department of the Interior's Mineral Institute's program administered by the Bureau of Mines under Allotment Grant Nos. G1124149, G1134149, and G1144149 and by the National Science Foundation under Grant No. INT 82-11631.

REFERENCES

1. H.M. Harris, A.W. Henderson, and T.T. Campbell: U.S. Bureau of Mines, Rep. Invest. 8165, 1976, 19 pp.
2. G.W. Elger, J.E. Tress, and R.R. Jordan: *Light Met.*, 1982, pp. 1135-47.
3. B.P. Judd and E.R. Palmer: *Proc. Australas. Inst. Min. Metall.*, 1973, vol. 247, pp. 23-33.
4. M.H. Tikkanan, T. Tyynela, and E. Vuoristo: *Met. Soc. Conf.*, 1964, vol. 24, pp. 269-82.
5. J.A. Kahn: *J. Met.*, 1984, vol. 36 (7), pp. 33-38.
6. W.E. Dunn, Jr.: *Trans. AIME*, 1960, vol. 218, pp. 6-12.
7. A.J. Morris and R.F. Jensen: *Metall. Trans. B*, 1976, vol. 7B, pp. 89-93.
8. A. Bergholm: *Trans. AIME*, 1961, vol. 221, pp. 1121-29.
9. M. Ogawa, M. Aso, and H. Mitsunami: *World Mining and Metal Technology*, 1979, pp. 1937-45.
10. A.A. Rabie, M.Y. Saada, and S.Y. Ezz: *Proc. Symp. of Inst. Min. Metall.*, 1968, pp. 501-05.
11. G.W. Elger, J.B. Wright, J.E. Tress, H.E. Bell, and R.R. Jordan: U.S. Bureau of Mines, Rep. Invest. 9002, 1986, 24 pp.
12. K.I. Rhee and H.Y. Sohn: *Metall. Trans. B*, 1990, vol. 21B, pp. 321-30.
13. K.I. Rhee and H.Y. Sohn: *Metall. Trans. B*, 1990, vol. 21B, pp. 331-40.
14. A.W. Nienow, P.N. Rowe, and L.Y. Cheung: *Powder Technol.*, 1978, vol. 20, pp. 89-97.
15. H.Y. Sohn: *Metall. Trans. B*, 1978, vol. 9B, pp. 89-96.
16. D.M. Himmelblau: *Applied Nonlinear Programming*, McGraw-Hill, Inc., New York, NY, 1972, pp. 149-57.